



HAL
open science

Phase transformation and damage elastoplastic multiphase model for welding simulation

Tong Wu, Michel Coret, Alain Combescure

► **To cite this version:**

Tong Wu, Michel Coret, Alain Combescure. Phase transformation and damage elastoplastic multiphase model for welding simulation. The 16th European Conference of Fracture, Jul 2006, Alexandroupolis, Grèce. pp.149-160, 10.1007/1-4020-5329-0_13 . hal-00506866

HAL Id: hal-00506866

<https://hal.science/hal-00506866v1>

Submitted on 3 Dec 2024

HAL is a multi-disciplinary open access archive for the deposit and dissemination of scientific research documents, whether they are published or not. The documents may come from teaching and research institutions in France or abroad, or from public or private research centers.

L'archive ouverte pluridisciplinaire **HAL**, est destinée au dépôt et à la diffusion de documents scientifiques de niveau recherche, publiés ou non, émanant des établissements d'enseignement et de recherche français ou étrangers, des laboratoires publics ou privés.



Distributed under a Creative Commons Attribution - NonCommercial 4.0 International License

PHASE TRANSFORMATION AND DAMAGE ELASTOPLASTIC MULTIPHASE MODEL FOR WELDING SIMULATION

T. WU, M. CORET, AND A. COMBESURE

LaMCoS, CNRS UMR 5514, National Institute of Applied Sciences, Lyon
20 av A. Einstein, 69621 Villeurbanne Cedex, France

Tong.wu@insa-lyon.fr, Michel.coret@insa-lyon.fr,
Alain.combescure@insa-lyon.fr

ABSTRACT

The aim of the article is to study and develop welding numerical models in the phase transformation and damage condition. The models are based on the study of damage concept in the multiphasic behavior, which occurs by welding process. The core of models or constitutive equations is the coupling between ductile damage, small strain elasticity, finite visco-plasticity and phase transformation. Based on the theory of thermodynamics and continuum damage mechanics (CDM), constitutive equations are built to describe damage growth and crack appearance during and after welding. The thermodynamics of irreversible processes with state variables is used as a framework to develop the phase coupling model. The related numerical aspects concern both the local integration scheme of the constitutive equations and the global resolution strategies. In this study, the majority of efforts are devoted to the theoretical developing of damage model. In addition, the models are implemented in computing software MATLAB[®] and CEA CAST3M[®] finite element code, and some calculations are presented to further explain the models in the end of the article.

Introduction

Under certain conditions, damage and phase transformation phenomenon exist simultaneously during welding process. For example, the welding of 16MND5 (French nuclear ferrite steel) or 15Cr-5Ni (martensitic stainless steel) components in the manufacture of nuclear equipment produces phase transformation phenomenon during heating and cooling stages, while damages induced by welding usually happen during cooling stage of welding. It means that mechanics properties of components or structures are affected by damage or even fracture induced by welding. Thus, it is really significative to use numerical modeling method to analysis and predict welding results, including the distribution of residual stress and damage. According to numerical results, the adjustments of the process parameters are implemented before doing the real experiments and manufacture processes in order to save time and money. However, now there is no evidence of a model that is able to predict the damage induced by welding process. One observes high spatial and temporal gradients as well as phase transformations. Such situations imply to cope with a diversity of damage models and add complexity to standard constitutive equations. The model contains three main ingredients: continuum damage mechanics, transformation plasticity and multiphase behavior. A graphic representation of these coupling mechanisms (Figure 1) was given

by Inoue [1]. Although some authors proposed to take all these phenomena into account in a common framework, we consider the influences of mechanics on thermics (arrow No. 4) and of mechanics on metallurgy (arrow No. 6) as second-order effects, since it has been observed that for such steels the influence of the stress state on the transformation diagrams is small. This assumption enables us to solve the thermometallurgical problem independently of the mechanical one. M. Coret and A. Combescure have done some work about such coupling mechanical behaviors under without damage condition [2-5]. Our study of damage factor coupling with other thermometallurgical and mechanical problems is based on their previous work.

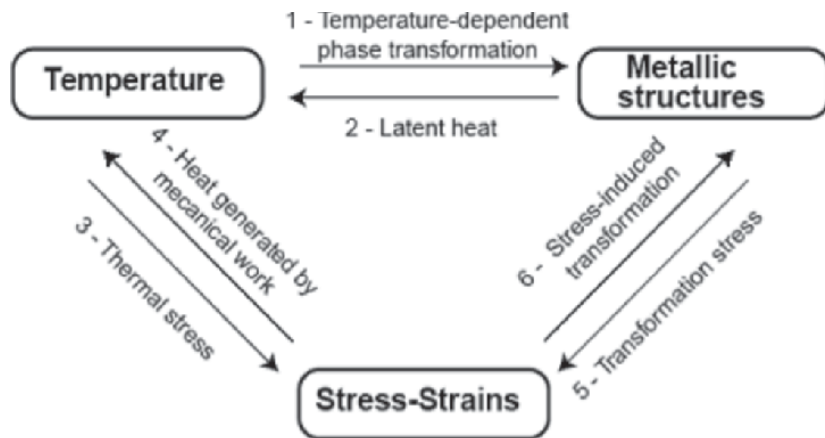


Figure 1. Coupling mechanisms [1]

To model the behavior of damage of continuous medium, the modeling of the damage can be done according to two different approaches. One rests on a micromechanical approach whereas the other uses a phenomenological macroscopic one.

The micromechanical approach uses the method of localization-homogenization, which makes it possible to go down on smaller scales from the structure (grain, system of slip) to describe the elementary mechanisms of the damage. For this micromechanical aspect, mechanisms are to be implemented in order to determine the required sizes. For example, the process of homogenization consists in determining the macroscopic sizes of volume representative element from those of basic cells by taking suitable averages. Although such an approach seems to be closer to reality of material, it is not easily realizable for the metal structural calculation. The computing time is extremely long because of the number considerable of equations.

The other approach of modeling is purely phenomenologic. It is founded on the introduction of variables of state associated with the various phenomena revealed by the experimentation. These phenomena are described within the framework of the thermodynamics of the irreversible processes [6]. There are still two approaches, which can be underlined. One is gained through physical inspiration. GURSON, ROUSSELIER, GELIN, BENNANI, PICART and others developed certain such kinds of models. The other comes from phenomenologic and macroscopic inspiration: KACHANOV, RABOTNOV, CHABOCHE and LEMAITRE built up this kind of damage model. The physical approach is based on a growth rate of the cavities inside a matrix with the elastoplastic behavior. By construction, this theory supposes the isotropy of the damage and uses a scalar variable to describe the volume fraction of the cavities.

Definition of Damage

The theory of the continuum damage mechanics is based on the assumption of the difference of scale between the micro-damage (microcracks and microvoids) and the Representative Volume Element (RVE). The damage analysis gives criteria for the creation of mesocracks, and then fracture mechanics is used to describe the phenomena. It is important to use a unique formulation to describe the different damage processes. It is based on the assumption that damage is driven by plastic strains, elastic strain energy and by an instability process. The macroscale scalar variable is defined to describe damage [7, 8]:

$$D = \frac{S_D}{S} \quad (1)$$

where S is the original surface, and S_D is the damaged surface.

$D = 0$: Undamaged material

$D = 1$: Fully broken material in parts

$0 < D < 1$: Failure occurs but crack does not happen

In the model, it is important and clearly understood to adopt the unique macro variable to describe the damage phenomena. Such damage macro variable is obtained through two approaches: 1) to integrate the unique micro damage variable (regard no difference between the damage in the austenitic phase and one in the martensitic phase); 2) to unify two micro damage variable (the ductile damage of the austenitic phase and the ductile damage of the martensitic phase) into one damage variable. For phase-transformation material, such as martensite stainless steel, there exist both martensitic phase and austenitic phase simultaneously during the specific heating or cooling stages. In order to closer the reality, it is necessary to describe the two different phases respectively. The Representative Volume Element (RVE) and microdamage are two scales of materials. In fact, the RVE consists of inclusions and matrix (the austenitic phase and the martensitic phase), and microdamage (microcracks and microvoids) distribute in inclusions and matrix (Figure 2). In our model, the damage in the inclusions (martensite) is regarded different from damage in the matrix (austenite). The damage in martensitic phase is marked by D_α , and the damage in austenitic phase is noted by D_γ . In microscale approach, the local damage variable at one point is defined by:

$$D_\mu = \frac{dS_D}{dS} \quad (2)$$

And the macroscale variable of damage can be given and developed by microscale definition of damage one.

$$\begin{aligned} D &= \frac{S_D^\gamma}{S} + \frac{S_D^\alpha}{S} = \frac{1}{S} \int_{S^\gamma} dS_D + \frac{1}{S} \int_{S^\alpha} dS_D = \frac{1}{S} \int_{S^\gamma} D_\mu dS + \frac{1}{S} \int_{S^\alpha} D_\mu dS \\ &= D_\alpha \xi_s + D_\gamma (1 - \xi_s) \end{aligned} \quad (3)$$

where ξ_s is the surface fraction of martensitic phase.

It was known that the damage variable is defined and deduced from the surface fraction, while the phase fraction of material is defined by the volume fraction. Therefore, in order to derive the constitutive equations of damage in phase transformation, we set up a bridge between both of them by formula:

$$D = D_\alpha \xi_s + D_\gamma (1 - \xi_s) = D_\alpha \xi_V^{2/3} + D_\gamma (1 - \xi_V^{2/3})$$

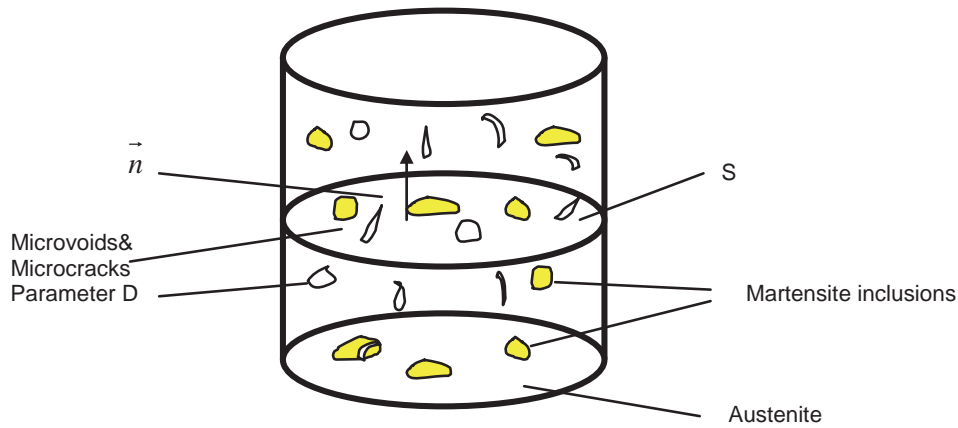


Figure 2. Damage variable and RVE

Phase transformation

The phase transformations often play a dominating role in the modeling of certain thermomechanical problems. Solid-state phase transformation causes the macroscopic geometric change because these different types of crystalline structures have different densities, which is so-called transformation-induced volumetric strain. This deformation can be explained by two micromechanical mechanisms of Greenwood and Johnson and of Magee. The transformations are strongly dependent not only on the speed of cooling but also on the composition in elements of alloys. Two types of diagrams are used by the researchers of the heat treatments to represent these transformations simply: Time-temperature transformation (TTT) diagrams are obtained by fast cooling of austenite then maintenance at constant temperature; continuous cooling transformation (CCT) diagrams represents the transformations during cooling at constant speed. In our research, we focus on the transformation from austenite to martensite after welding. The martensitic transformation should be treated separately comparing other transformations, because it was considered as independent of time. The empirical law of Koistinen and Marburger gives the voluminal fraction of martensite according to the temperature. The theoretical justification of this equation was given by Magee:

$$z_{\alpha} = z_{\gamma} (1 - e^{-\beta(M_s - T)}) \quad (4)$$

where z_{α} and z_{γ} are voluminal proportion of martensite and austenite respectively; M_s is martensite start temperature; β is coefficient depend on material; T represents temperature.

On the one hand, from a mechanical point of view, the phase transformations are complex phenomena that induced constraints growth or release. On the other hand, the application of pressure modified both the energy stored in material and the structure of the material, and caused the deformation's changes in macroscale (Figure 3). Therefore, the influence of the stress on the transformations of phases can not be neglected to some extent. It was shown that extremely high pressures about the hundreds MPa lead to notable effects on the kinetics of transformations [9]. Further more, even a low macroscopic constraint applied, lower than the yield stress of the softest phase, an additional deformation, called "Transformation-Induced Plasticity" (TRIP), can be

observed during the transformation (Figure 4). Leblond's transformation plasticity model [10,11,12] is presented to further explain the TRIP as follows:

$$\dot{E}^{pt} = -\frac{3\Delta\varepsilon_{\gamma-\alpha}^{th}}{\sigma_{\gamma}^y} \cdot S \cdot h\left(\frac{\Sigma^{eq}}{\Sigma^y}\right) \cdot (\ln z) \cdot \dot{z} \quad (5)$$

$\Delta\varepsilon_{\gamma-\alpha}^{th}$: Difference of thermal deformations between the two phases.

Σ^{eq} : Macroscopic von Mises equivalent stress.

Σ^y : Homogenized ultimate stress.

z : Volume proportion of phase α .

S : Deviator of the macroscopic stress.

$h\left(\frac{\Sigma^{eq}}{\Sigma^y}\right)$: Term that translates the non-linearity of the plasticity of

transformation, defined by:

$$h\left(\frac{\Sigma^{eq}}{\Sigma^y}\right) = \begin{cases} 1, & \text{if } \frac{\Sigma^{eq}}{\Sigma^y} \leq \frac{1}{2} \\ 1 + \frac{7}{2}\left(\frac{\Sigma^{eq}}{\Sigma^y} - \frac{1}{2}\right), & \text{if } \frac{\Sigma^{eq}}{\Sigma^y} > \frac{1}{2} \end{cases}$$

For most situations, the following simplified formulation also leads to content effects:

$$\dot{E}^{pt} = -\frac{3\Delta\varepsilon_{\gamma-\alpha}^{th}}{\sigma_{\gamma}^y} \cdot S \cdot (\ln z) \cdot \dot{z} \quad (6)$$

The equivalent TRIP strain can be gained from the integral of the TRIP' rate:

$$E_{eq}^{pt} = \int_{t_0}^{t_1} \dot{E}^{pt} dt = -\int_{t_0}^{t_1} \frac{3\Delta\varepsilon_{\gamma-\alpha}^{th}}{\sigma_{\gamma}^y} \cdot S \cdot (\ln z) \cdot \dot{z} dt \quad (7)$$

If we consider that $\Delta\varepsilon_{\gamma-\alpha}^{th}$ is constant and the cooling rates of different time keep same during the transformation, we have:

$$E_{eq}^{pt} = IS = \frac{2}{3} I \sigma_{eq} \quad (8)$$

with

$$I = -3\Delta\varepsilon_{\gamma-\alpha}^{th} \int_{t_0}^{t_1} \frac{1}{\sigma_{\gamma}^y} \cdot (\ln z) \cdot \dot{z} \cdot dt = \text{Const (positive)}$$

This equation shows the direct relationship between the equivalent TRIP strain and the equivalent stress: the transformation-induced plastic strain is proportional to the level of the equivalent stress in von Mises' sense. Furthermore, in the case of small loads, the strain is proportional to the applied stress [3].

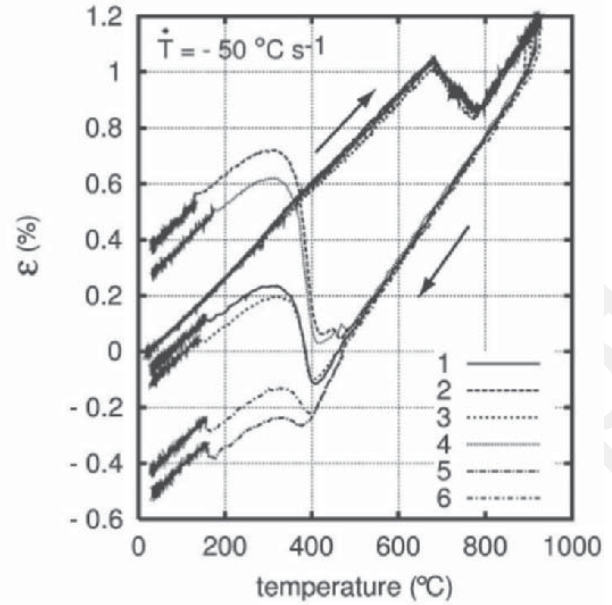
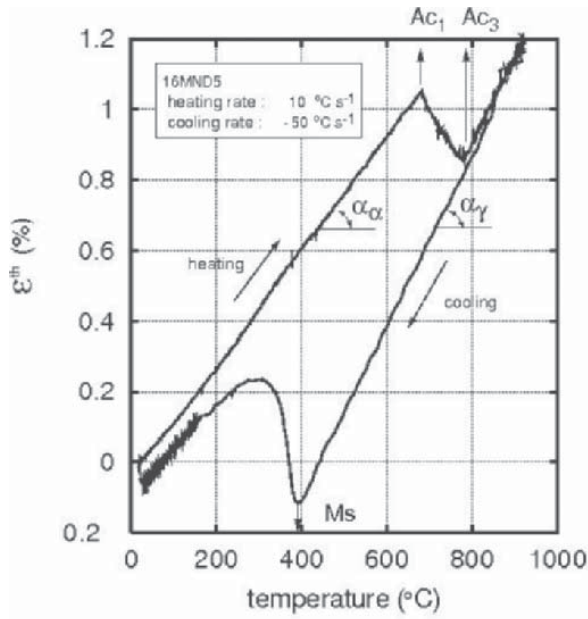


Figure 3. Free dilatometries of martensitic transformation [3]

Figure 4. Total strain with loading ($\sigma = 70MPa$) [3]

Mesoscopic Damage Model

The mesoscopic model, which we introduced, is much more numerically oriented and ignores a priori constitutive law for each phase, and it developed based on the method of localization-homogenization. The homogenizing procedure used is the Taylor's localization law, which assumes homogeneous deformations in a heterogeneous medium with nonlinear behavior. This law provides the closest possible match with Leblond's theoretical case for elastoplastic phases. Such approach, called micro-macro, consists of starting from the behavior of each phase and working back to the macroscopic behavior of the material. After the localization, the behavior of each phase can be treated respectively, without coupling. Such model provides the freedom to choose the behavior type of each phase. It seems more reasonable not only to adopt different material properties but also to use the different types of behaviors for the austenitic and martensitic phases. Therefore, as other behaviors, our mesoscopic damage model adopts two damage variables corresponding to phase α and phase γ to further describe the damage during the phase transformation between martensite and austenite.

We suppose that the material have two types solid solution: α type solid solution and γ type solid solution. The martensite, ferrite and bainite have the same α type solid solution while the austenite is γ type solid solution. In this model, we use martensitic phase to replace other α type phases. We adopt the following variables for the fraction of phase: z_α is the volume fraction of phase α . And then, the volume fraction of phase γ is z_γ . In addition, we regard that the damage in the α phase D_α is different from that in the γ phase D_γ , and D_α is no coupling with D_γ . The approach was based on the Voigt model with equal repartition of strains in all phases of the multiphase composite.

$$\varepsilon = \varepsilon_i \quad (i = \alpha, \gamma) \quad (9)$$

Based on the principle of localization mentioned above, we split the total strain ratio into two parts, one coming from the total microscopic strain rate of the phases, and the other representing the plastic transformation strain rate. Thus:

$$\dot{E}^{tot} = \dot{\varepsilon} + \dot{E}^{pt} \quad (10)$$

In our model, classical plasticity and transformation plasticity are assumed to be uncoupled, which is true for small strain. Thus, the homogenization law for stress is:

$$\underline{\Sigma} = \sum_{i=\alpha,\gamma} z_i \underline{\sigma}_i \quad (11)$$

In addition, the homogenization law for damage is presented in Equation 4.

Such modeling scheme provides great flexibility in the calculation. Thus, arbitrary constitutive laws, including different models of transformations plasticity rates and damage governing equations can be selected for each phase. Therefore, the equations of the mesomodel can be developed as follows.

The strain equations are:

$$\dot{E}^{tot} = \dot{\varepsilon} + \dot{E}^{pt} \quad \forall i \quad (12)$$

$$\dot{\varepsilon}_i = \dot{\varepsilon}_i^e + \dot{\varepsilon}_i^{thm} + \dot{\varepsilon}_i^{vp} \quad \forall i \quad (13)$$

The transformation plasticity strain rate is given by Equation 6.

For each phase's behavior, various behavioral models were tested. Here, in order to focus on the interpretation of various coupling behavior clearly, we choose the same type of plastic hardening model (including isotropic and kenimatic hardening) for two phases, although adopting different models for each phase is closer to the reality. Material properties, including the damage parameters, should choose different data according to the various phase materials.

The elastic and thermometallurgical strains are:

$$\dot{\varepsilon}_i^e = H^{-1}(T) \underline{\sigma}_i + [\varepsilon_i^{thm}(T) - \varepsilon_i^{thm}(T_{ref})] \quad (14)$$

with

$$\varepsilon_i^{thm} = \alpha_i(T) \cdot TI \quad \text{for } \gamma \text{ phase}$$

$$\varepsilon_i^{thm} = \alpha_i(T) \cdot TI + z_\alpha \Delta \varepsilon_{\alpha-\gamma}^{T_{ref}} \quad \text{for } \alpha \text{ phase}$$

Our coupling model for each phase is developed on the base of method of local state in the thermodynamics of irreversible process [8, 9]. The various state's laws of the phases can deduced from the state potential of each phase and the partial differentials of each phase's pseudo-potential also can lead to flux variables. The totally internal energy e^{tot} consists of elastic and thermometallurgic internal energy $e^{e-th-met}$, viscoplastic (including isotropic and kenimatic hardening) internal energy $e^{vpj-vpk}$, and internal energy induced by phase-transformation e^{tr} as the following equation shown:

$$e^{tot}(\underline{\varepsilon}^e, T, p, \underline{\alpha}, D, z) = e^{e-th-met}(\underline{\varepsilon}^e, T, D, z) + e^{vpj-vpk}(T, p, \underline{\alpha}, D, z) + e^{tr}(T, z) \quad (15)$$

After the partial differential of the internal energy, the state relations (isotropic strain hardening variable R_i , back stress \underline{X}_i , release ratio of elastic energy $-Y_i$) for each phase are:

$$R_i = \frac{\partial e_i^{tot}}{\partial p_i} = c_i(T)(1-D_i)[1 - \exp(-\gamma_i p_i)] \quad (16)$$

$$\underline{X}_i = \frac{\partial e_i^{tot}}{\partial \underline{\alpha}_i} = \frac{2}{3} g_i(T) b_i (1-D_i) \underline{\alpha}_i \quad (17)$$

$$-Y_i = \frac{\partial e_i^{tot}}{\partial D_i} = \frac{1}{2} A_i(T) \underline{\varepsilon}_i^e : \underline{\varepsilon}_i^e + \frac{1}{3} g_i(T) b_i \underline{\alpha}_i : \underline{\alpha}_i + c_i(T) \left[p_i + \frac{1}{\gamma_i} \exp(-\gamma_i p_i) \right] \quad (18)$$

The pseudo-potential of dissipation φ_i is the function of all the dual variables:

$$\varphi_i = \varphi_i(\underline{\sigma}_i, A_k, \overrightarrow{\text{grad}T}, Y_i, k; \underline{\varepsilon}^e, V_k, T, D_i) \quad (19)$$

The damage potential φ_i^D can be defined by:

$$\varphi_i^D = \frac{S_i}{(s_i + 1)(1-D_i)} \left(\frac{-Y_i}{S_i} \right)^{s_i+1} \quad (20)$$

S_i and s_i : Characteristic coefficients of materials to describe damage, usually are the functions of temperature.

The yield function of each phase can be written:

$$f_i = f_i(\underline{\sigma}_i, R_i, \underline{X}_i, D_i) = \frac{J_2(\underline{\sigma}_i - \underline{X}_i)}{\sqrt{1-D_i}} - \frac{R_i}{\sqrt{1-D_i}} - \sigma_{yi} \quad (21)$$

then

$$F_i = f_i + \frac{a_i}{2(1-D_i)} J_2^2(\underline{X}_i) + \frac{b_i}{2(1-D_i)} R_i^2 + \frac{S_i(T)}{[s_i(T)+1](1-D_i)} \left[-\frac{Y_i}{S_i(T)} \right]^{s_i(T)+1} \quad (22)$$

σ_{yi} : The yield stress of phase i .

The whole of the selected variables and the potentials previously defined lead to a thermodynamically acceptable model whose general formulation is presented as follows.

The viscoplastic flow:

$$\underline{\dot{\varepsilon}}_i^p = \frac{\partial \varphi_i}{\partial \underline{\sigma}_i} = \frac{3}{2} \frac{\dot{p}_i}{\sqrt{1-D_i}} \frac{\underline{\sigma}_i^D - \underline{X}_i^D}{J_2(\underline{\sigma}_i - \underline{X}_i)} \quad (23)$$

The evolution of the internal variable associated with isotropic hardening:

$$\dot{r}_i = -\frac{\partial \varphi_i}{\partial R_i} = u_i \langle F_i \rangle^{n_i} \quad (24)$$

The evolution of the internal variable associated with kinematic hardening:

$$\dot{\underline{\alpha}} = -\frac{\partial \varphi_i}{\partial \underline{X}_i} = \frac{3}{2} \frac{\dot{p}_i}{\sqrt{1-D_i}} \frac{\underline{\sigma}_i^D - \underline{X}_i^D}{J_2(\underline{\sigma}_i - \underline{X}_i)} \quad (25)$$

The evolution of the damage variable:

$$\dot{D}_i = -\frac{\partial \varphi_i}{\partial Y_i} = \frac{S_i}{(1-D_i)} \left(\frac{-Y_i}{S_i} \right)^{s_i} \quad (26)$$

Numerical Analysis

As far as the numerical analysis is concerned, the first step is to computer the coupled transient temperature and metallurgical phase field. The second one is stress and strain field computation and then the states of each phase (stresses, strains, internal variables, damage ...) are output. At the end, we can homogenize the strains and stresses, displacements and damages.

In order to explain the models, we give elementary calculations of examples in this part. These calculations are implemented in Matlab 6.5, and they can illustrate directly the damage evolution and other coupling behaviors.

Here, we introduce the ‘‘Satoh’’ type test that an uniaxial bar is clamped on the top and bottom and simultaneously suffer thermal loading. The test consists of austenitizing and martensitizing with cooling homogeneously a test piece whose longitudinal displacements are restrained. Thus can be used to induce the same or similar phenomena as that can be observed in welding heat-affected zone (HAZ). This led us to choose this type of test in the framework of this study for the analysis. The test contains several complex coupled phenomena, and they are thermal (temperature), metallurgical (phase-transformation) and mechanical (strain-stress, damage) behaviors.

In our calculation, the total strain is partitioned as follows (for Satoh test, $E^{tot} = 0$):

$$E^{tot} = E^e + E^{thm} + E^{pc} + E^{pt} \quad (27)$$

where E^e is the macroscopic elastic strain, E^{thm} is the macroscopic thermo-metallurgical strain, E^{pc} is the classical macroscopic plastic strain and E^{pt} is the transformation-induced-plasticity strain.

$$E^{thm} = [z_\gamma \alpha_\gamma + z_\alpha \alpha_\alpha] (T - T^{T_{ref}}) + z_\gamma \Delta \varepsilon_{\alpha\gamma}^{T_{ref}} \quad (28)$$

where $T_{ref} = 20^\circ C$

Thermal strain difference between the two phases: $\Delta \varepsilon_{\alpha\gamma}^{20^\circ C} = 0.011$

Thermal expansion coefficient of the austenitic phase ($T_{ref} = 1000^\circ C$):

$$\alpha_\gamma = 22.6 \times 10^{-6} + 2.52 \times 10^{-9} \cdot T$$

Thermal expansion coefficient of the martensitic phase:

$$\alpha_\alpha = 12.35 \times 10^{-6} + 7.71 \times 10^{-9} \cdot T (T \leq 350^\circ C); \alpha_\alpha = 15 \times 10^{-6} (350^\circ C < T < 700^\circ C)$$

The beginning temperature of martensitic transformation: $M_s = 400^\circ C$

We suppose the bar has the elasticity and perfect plasticity that the Young's modulus and yield stress depend on temperature, which is given in Table 1. The temperature loading of the bar is from $1000^\circ C$ to $20^\circ C$ with $\dot{T} = 9.8^\circ C/s$. The phase-transformation model adopts Magee's model as shown in Equation 5 and Figure 5. The martensitic phase transformation occurs at temperature $400^\circ C$ and the proportion of austenitic

phase quickly increases, near to 0 at ambient temperature. The TRIP, related to macroscopic stress, is calculated according to Leblond's model (Equation 6).

T (°C)	0	100	200	400	600	700	800	900	1000
E (GPa)	208	204	200	180	135	80	50	32	30
σ_{ym} (MPa)	1200	1170	1100	980	680	350	100	50	20
σ_{ya} (MPa)	140	130	120	110	100	70	60	30	20

m=martensite, a=austenite

Table 1. Material properties

It is generally accepted that the additional flow induced by the TRIP strain plays a significant role in the evolution of the stress during structural transformations. Our results can verify this point and various strains are presented in Figure 6. The TRIP strain is dominating comparing others, and such big value is because of the large macroscopic stress at low temperature. Furthermore, the TRIP strain that comes from the damage-mechanical model is smaller a little than one gained from the usual strain-stress model (without damage) because of the decline of stress in damage condition. Although TRIP notably affects the stress via changing elastic stress in elastic stage, it changes the stress little in plastic stage because of perfect plasticity. In fact, the thermal strain has observable effect to the stress in "Sato" test, but the metallurgical stain from austenite to martensite weakens this effect because its volume increases whereas the thermal strain is negative.

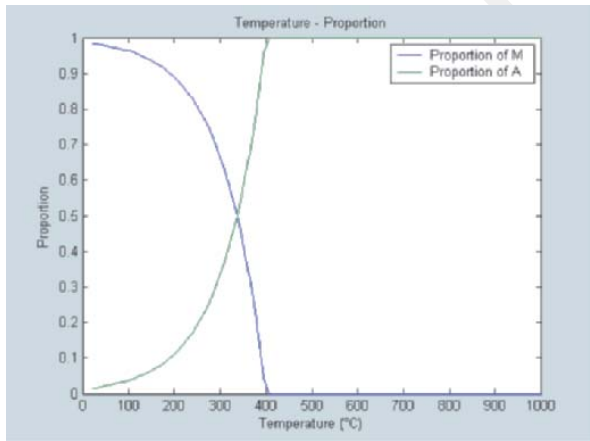


Figure 5. Proportion of each phase

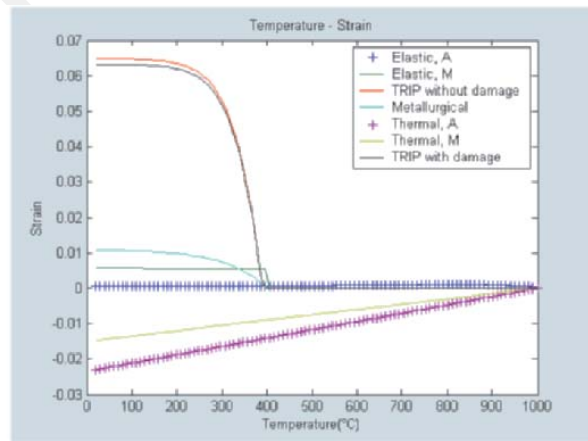


Figure 6. Various strains vs. temperature

From the Figure 7, it is observed that both austenite and martensite are yield at the beginning of their existed stage (martensite, near to 400°C). Generally, the austenitic component of stress is much lower than the martensite's because of the big difference of yield stresses. It is evident that damage decreases the effective stress, especially for martensitic component. For austenitic component, it is not large effect whether coupling damage or not. Thus is caused by its smaller damage variable (Figure 8). Before phase transformation, the all variables of martensite equal to zero and the mechanical behavior is entirely predominated by single austenitic phase. With the development of phase transformation, the martensite plays more and more role not only in evolution of stress

but also to the damage's growth. At the end of phase-transformation stage, the macroscopic stress increases slowly or even decreases because of damage's effect.

In this calculation, there are lacking for accurate material data about damage because the calibration test is still going on and can be finished soon. However, the numerical results give an interesting in-depth insight about complicated phenomena coupling with damage.

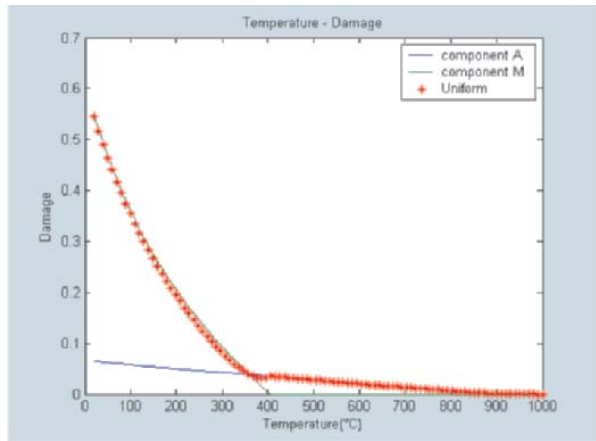
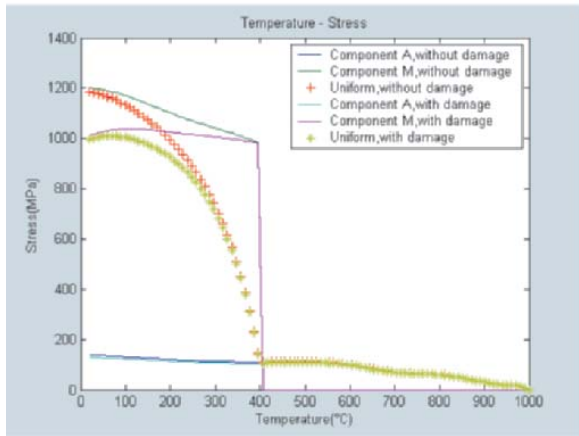


Figure 7. Comparing stress with/without damage Figure 8. Damage variables

Conclusion and prospective

The objective of this study is to develop the damage model to describe damage during the cooling in welding process, and it was accomplished in the aspect of theoretical derivation. Comparing the traditional model of damage, which does not take the phase transformation into account, our new mesoscopic damage model has its own advantage: it is free to choose the behavior for each phase whereas it is difficult or impossible to choose the reasonable parameters for various-phase material through traditional model.

The model coupled thermal, metallurgical and mechanical behaviors can be used to predict not only the strain and stress fields but also the damage distribution in welded work piece. In fact, the numerical results, especially stress, through the coupled damage model, are closer to material's state than that through the model coupled without damage.

The specific test of "Sato" type is adopted to imitate the real welding process as a matter of simplification. In this case, virtually all the thermo-mechanical and thermo-metallurgical phenomena, which can be observed in the HAZ, are present simultaneously. For that reason, the Sato tests are very useful in validating the constitutive relations used to describe the mechanical evolution in the HAZ.

The comparative analyses of the calculations and the experiments should be implemented after the completeness of calibration test of damage and welding damage experimental.

Acknowledgments

This research is one part of project INZAT4 sponsored by EDF-SEPTEN, FRAMTOME-ANP, ESI-GROUP, EADS-CCR, Rhône-Alps, and INSA-Lyon, so we thank their financial and technical supports.

References

1. Inoue T, Wang Z. Coupling between stress, temperature, and metallic structures during processes involving phases transformations. *Materials Science and Technology*, 1: 845–50,1985.
2. Coret, M., Etude expérimentale et simulation de la plasticité de transformation et du comportement multiphase de l'acier de cuve 16MND5 sous chargement multiaxial anisotherme, These, LMT-Cachan, Paris, France, 2001.
3. Coret, M., Calloch, S. and Combescure, A., Experimental study of the phase transformation plasticity of 16MND5 low carbon steel induced by proportional and nonproportional biaxial loading paths, *European Journal of Mechanics - A/Solids*, vol. 23, 823-842, 2004.
4. Coret, M., Calloch, S. and Combescure, A., Experimental study of the phase transformation plasticity of 16MND5 low carbon steel under multiaxial loading, *International Journal of Plasticity*, vol. 18, 1707-1727, 2002.
5. Coret, M., and Combescure, A., A mesomodel for the numerical simulation of the multiphase behavior of materials under anisothermal loading, *International Journal of Mechanical Sciences*, vol. 44, 1947-1963, 2002.
6. Germain, P., Nguyen, Q.S., Suquet, S., *Continuum thermodynamics*, *J. Applied Mechanics*, ASME, vol. 50, 1010-1020, 1983.
7. Chaboche, J.L., Description thermodynamique et phénoménologique de la viscoplasticité cyclique avec endommagement, Thèse de Doctorat Es-Science, Paris, VI, 1978.
8. Lemaitre, J. and Chaboche, J. L., *Mechanics of Materials*, Cambridge University Press, Cambridge, 1994.
9. Aliage, C., Massoni, E., Louin. J.C., and Denis. S., 3D finite element simulation of residual stresses and distortions of cooling workpieces. In 3rd international conference on quenching and control of distortion, Prague, Czech Republic, 1999.
10. Leblond, J., Devaux, J., Devaux, J., Mathematical modelling of transformation plasticity in steel i. case of ideal-plastic phases. *Int. J. Plasticity* 5, 551–572, 1989.
11. Leblond, J., Devaux, J., Devaux, J., Mathematical modelling of transformation plasticity in steel i. coupling with strain hardening phenomena. *Int. J. Plasticity* 5, 573–591, 1989.
12. Vincent, Y., Jullien, J.F., Gilles, P., Thermo-mechanical consequences of phase transformation in the heat-affected zone using a cyclic uniaxial test, *International Journal of Solid and Structures*, Elsevier Ltd, 4077-4098, July 2005.